Multilevel Cancer Modeling in the Clinical Environment: Simulating the Behavior of Wilms Tumor in the Context of the SIOP 2001/GPOH Clinical Trial and the ACGT Project

Eleni Ch. Georgiadi, Georgios S. Stamatakos, Norbert M. Graf, Eleni A. Kolokotroni,
Dimitra D. Dionysiou, Alexander Hoppe, Nikolaos K. Uzunoglu, *Senior Member IEEE*

Abstract—Mathematical and computational tumor dynamics models can provide considerable insight into the relative importance and interdependence of related biological mechanisms. They may also suggest the existence of optimal treatment windows in the generic setting. Nevertheless, they cannot be translated into clinical practice unless they undergo a strict and thorough clinical validation and adaptation. In this context one of the major actions of the EC funded project "Advancing Clinico-Genomic Trials on Cancer" (ACGT) is dedicated to the development of a patient specific four dimensional multiscale tumor model mimicking the nephroblastoma tumor response to chemotherapeutic agents according to the SIOP 2001/GPOH clinical trial. Combined administration of vincristine and dactinomycin is considered. The patient's pseudoanonymized imaging, histopathological, molecular and clinical data are carefully exploited. The paper briefly outlines the basics of the model developed by the *In Silico* Oncology Group and particularly stresses the effect of stem/clonogenic, progenitor and differentiated tumor cells on the overall tumor dynamics. The need for matching the cell category transition rates to the cell category relative populations of free tumor growth for an already large solid tumor at the start of simulation has been clarified. A technique has been suggested and succesfully applied in order to ensure satisfaction of this condition. The concept of a *nomogram* matching the cell category transition rates to the cell category relative populations at the treatment baseline is introduced. Convergence issues are addressed and indicative numerical results are presented. Qualitative agreement of the model's behavior with the corresponding clinical trial experience supports its potential to constitute the basis for an optimization system within the clinical environment following completion of its clinical validation and optimization. *In silico* treatment experimentation in the patient individualized context is expected to constitute the primary application of the model.

I. INTRODUCTION

Apart from a disease cancer is a highly complex and multiscale *natural phenomenon.* Over the last decades considerable efforts have been made in order to simulate tumor growth and response to various (chemo)therapeutic schemes so as to provide an analytical weapon for understanding and fighting the disease. In this context a Euro-Japanese effort to develop the "Oncosimulator" within the framework of the European Commission (EC) funded project "Advancing Clinico-Genomic Trials on Cancer" (ACGT) [1] is under way. The simulation module of this personalized treatment support system is based on the top-down approach being developed by the *In Silico* Oncology Group (www.in-silico-oncology.iccs.ntua.gr). The present paper deals with the paradigm of nephroblastoma (Wilms tumor) chemotherapeutically treated in the neoadjuvant setting according to the SIOP 2001/GPOH clinical trial which is addressed by ACGT [1-2]

II. A BRIEF OUTLINE OF THE SIMULATION MODEL

A. Tumor Initialization

1) Spatial Initialization

The anatomical region of interest is discretized using a cubic mesh. Each elementary cube of the mesh is called a *geometrical cell* (GC) [3-6] and is used as the spatial unit for the differential (local) description of the biological activity of an imageable tumor [7-10]. In this paper a spatially homogeneous tumor of ellipsoidal shape is considered as an initial approximation to a real Wilms tumor. This is a reasonable assumption since the triaxial ellipsoidal shape is extensively used in clinical practice e.g. in the Case Report Forms (CRFs) of the SIOP 2001/GPOH nephroblastoma clinical trial [1]. The center of the ellipsoid is considered to coincide with the center of the discretizing mesh. The

E. Ch. Georgiadi is with the National Technical University of Athens, Institute of Communication and Computer Systems, *In Silico* Oncology Group, Iroon Polytechniou 9, Zografos, GR-157 80, Greece (e-mail: egeorg@ics.forth.gr)and the Foundation for Research and Technology – Hellas, Institute of Computer Science, N. Plastira 100, Vassilika Vouton, GR-700 13 Heraklion, Crete, Greece

G. S. Stamatakos (corresponding author) is with the National Technical University of Athens, Institute of Communications and Computer Systems, *In Silico* Oncology Group, Iroon Polytechniou 9, Zografos, GR-157 80, Greece (phone: + 30 210 772 2288, fax: + 30 210 772 3557, e-mail: gestam@central.ntua.gr).

N.Graf is with the University Hospital of the Saarland, Paediatric Haematology and Oncology, D-66421 Homburg,, Germany (e-mail: norbert.Graf@uniklinikum-saarland.de   ).

E. A. Kolokotroni is with the National Technical University of Athens, Institute of Communication and Computer Systems, *In Silico* Oncology Group, Iroon Polytechniou 9, Zografos, GR-157 80, Greece (e-mail: ekolok@iccs.gr).

D. D. Dionysiou is with the National Technical University of Athens, Institute of Communications and Computer Systems, *In Silico* Oncology Group, Iroon Polytechniou 9, Zografos, GR-157 80, Greece (e-mail: dimdio@esd.ece.ntua.gr).

A.Hoppe is with the University Hospital of the Saarland, Paediatric Haematology and Oncology, D-66421 Homburg,, Germany (e-mail: Alexander.Hoppe@uniklinikum-saarland.de).

N.Uzunoglu is with the National Technical University of Athens, Institute of Communications and Computer Systems, *In Silico* Oncology Group, Iroon Polytechniou 9, Zografos, GR-157 80, Greece (e-mail: nnap@otenet.gr)

geometrical cells of discretizing mesh are initially considered occupied if they belong to the tumor mass.

2) Cell Population and Time Initialization

Each GC of the discretizing mesh can normally accomodate a number of biological cells (NBC). The typical cell density of 10^9 cells/cm^3 [9] is adopted. Therefore a GC of volume equal to 1 mm^3 is assumed to contain 10^6 (biological) cells (Table I). From the mitotic potential partition point of view within each GC the following *equivalence classes* (categories) of tumor cells are considered:

stem/clonogenic cells: cancer cells assumed to possess theoretically unlimited proliferative potential

limp (limited mitotic potential) or *progenitor cells:* cancer cells with limited mitotic potential. Three divisions are assumed before terminal differentiation occurs in the simulations presented in this paper. Other numbers of mitoses before differentiation can also be considered.

differentiated (diff) cells : terminally differentiated cells

necrotic cells: cells that have died through necrosis

apoptotic cells: cells that have died through apoptosis

Stem or limp cells can be proliferating or dormant (i.e. residing in the G0 cell cycle phase due to inadequate oxygen and/or nutrient supply). Proliferating stem and limp cells are further distributed into classes corresponding to the cell cycle phases in which they are (temporarily) residing. The following cell cycle phases are considered: G1 (Gap 1 phase), S (DNA synthesis phase), G2 (Gap 2 phase), M (Mitosis). The initial distribution of the proliferating cells to the various cell cycle phases is assumed proportional to the corresponding typical cell cycle phase durations. Based on [10] the following cell cycle phase durations (T_x) expressed as fractions of the total cell cycle duration (T_c) constitute a plausible assumption:

$$T_{G1} \approx 0.4 * T_c, \quad T_S \approx 0.39 * T_c, \quad T_{G2} \approx 0.19 * T_c,$$
$$T_M \approx 0.02 * T_c \tag{1}$$

Due to computer memory and/or performance limitations a number of quantizations of the biological system have to take place. Therefore all cells belonging to a given equivalence class within a GC are assumed to be synchronized. However, cells residing in different GCs or in different equivalence classes of the same GC are not considered synchronized. Use of a random number generator is made for this purpose. The discrete character of the simulation model enables the consideration of several exploratory initial percentages of the cells in the various equivalence classes.

An extensive study of the correlation between the cell category transition rates (e.g. percentage of the stem cell mitoses that are asymmetric) and the cell category relative populations (e.g. fractional population of the progenitor cells) for free tumor growth at the start of simulation has been performed. This correlation has led to the concept of the *nomogram* of cell category transition rates and cell category relative populations for a freely growing tumor (Section III). Since in the present paper macroscopically homogenous Wilms tumors have been considered all GCs are essentially initialized in the same. A small spatial perturbation of initialization is easily achieved through a (pseudo)random number generator. Macroscopically evident tumor inhomogeneities will be treated by a subsequent version of the model where pertinent algorithms already developed by our group [3-6] will also have been incorporated. In that case GCs belonging to macroscopically/metabolically different spatial regions of the tumor will be characterized by different initial cell category relative populations according to the imaging and other medical data.

B. Temporal Advancement of the Tumor System

1) Tumor Growth

All cells in all GCs follow the generic cytokinetic diagram shown in Fig.1 for the case of free tumor growth. This is a finite state construct that can be adjusted to any particular clinical case through assigning appropriate values to its parameters. According to Fig. 1 the following clusters of biological phenomena taking place at the cellular level of biocomplexity are taken into account: *cycling of the proliferating cells* through the cell cycle phases, *symmetric* and *asymmetric stem cell division*, *proliferation of limp (progenitor) cells* (n=3 divisions in the current version of the simulation code), *terminal differentiation* of progenitor cells, *spontaneous apoptosis*, *transition to the dormant (G0) phase* due to inadequate supply of oxygen and nutrients, *waking up of dormant cells* if the re is local reestablishment of oxygen and nutrient supply, *cell death through necrosis* (due to prolonged oxygen and nutrients shortage).
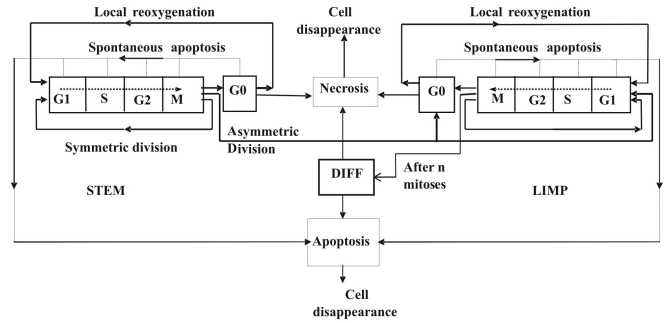

Fig. 1: Generic cytokinetic model for free tumor growth. STEM: stem cells. LIMP: limited proliferative potential (progenitor) cells. DIFF: terminally differentiated cells.

2) Tumor Response to Treatment

In order to tackle the tumor response to chemotherapy an extension of the cytokinetic diagram shown in Fig.1 is used. Thus cell death induced by a chemotherapeutic agent is introduced into the diagram. Cell cycle specific, cell cycle non specific, cell cycle phase specific and cell cycle non specific drugs can be readily simulated. For example by assigning the same drug induced death probability per hour to all cell cycle phases a cell cycle phase non specific drug action is modeled. On the other hand by assigning a high death probability per hour to a particular cell cycle phase a cell cycle phase specific drug action is modeled. Lethally hit

cells are assumed to enter a special cell cycle before ultimately dying.

The simulation algorithms developed so far address the cases of preoperative chemotherapy with a combination of actinomycin-D and vincristine for unilateral stage I-III nephroblastoma tumors treated according to the SIOP 2001/GPOH clinical trial in the framework of the ACGT project (Fig. 2).
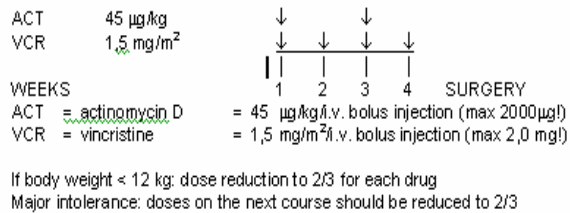


```
ACT     45 µg/kg           ↓        ↓
VCR     1,5 mg/m²      ↓   ↓   ↓   ↓

WEEKS                  │   │   │   │
                       1   2   3   4    SURGERY
ACT  = actinomycin D      = 45  µg/kg/i.v. bolus injection (max 2000µg!)
VCR  = vincristine        = 1,5 mg/m²/i.v. bolus injection (max 2,0 mg!)

If body weight < 12 kg: dose reduction to 2/3 for each drug
Major intolerance: doses on the next course should be reduced to 2/3
```

Fig. 2: The simulated Wilms tumor treatment protocol

3) Vincristine pharmacokinetics and pharmacodynamics

Following a vincristine intravenous (i.v.) bolus injection of 1.5 mg/m^2 the area under curve (AUC) is given according to [11] as equal to 6.7mg/L/min. According to [12] an experiment was carried out to test whether the arrest in metaphase of cervical carcinoma cells after treatment with various concentrations of vincristine for 6 hours was reversible. Treatment with 16×10^{-3} µg/ml of vincristine for 6 hours seems to produce an irreversible metaphase arrest and an AUC of 5.76 µg/ml/min =5.76 mg/L/min which is very close to the clinical AUC that has been observed in [11]. The metaphase index calculated at 90 min after the removal of the drug (a time period during which it increases) was equal to 240 (cells stuck in metaphase per 1000 cells). This value of 240/1000=0.24 can be considered to reflect the cell kill fraction in the experiment, since mitosis cannot be completed, the cell cycle cannot proceed and death should follow. As the value of 5.76 µg/ml/min for the AUC in this experiment is slightly lower than the clinical AUC value of 6.7 mg/L/min, a cell kill fraction equal to 0.3 could be justified as an initial gross approximation, which is expected to be corrected, if necessary, with the help of the ACGT clinical data. As a first approximation also the imperfect drug penetration into the tumor is assumed to have been taken into account in this value of 0.3 cell kill fraction.

The antineoplastic effect of vincristine is basically attributed to its ability to destroy the functionality of cell microtubules, which form the mitotic spindle, by binding to the protein tubulin [13]. Failure of the mitotic spindle results in apoptotic cell death at mitosis [14]. Vincristine is characterised as a cell cycle specific agent (exerts action on cells traversing the cell cycle) [10] and more specifically as an M-phase specific drug [13], [15]. Therefore, in the simulation model vincristine is assumed to bind at cells at all cycling phases and lead to apoptotic cell death at the end of M phase. It should be noted that vincristine cytotoxicity is known to decrease with increasing tumor cell density ("inoculum effect") [16].

4) Actinomycin-D (Dactinomycin) pharmacokinetics - pharmocodynamics

Actinomycin-D is a cell cycle-nonspecific antitumor antibiotic that binds to double-stranded DNA through intercalation between adjacent guanine-cytosine base pairs [10], thereby inhibiting its synthesis and function. It also acts to form toxic oxygen-free radicals, which create DNA strand breaks, inhibiting DNA synthesis and function. In the simulation model actinomycin-D is assumed to bind to cells at all cycling phases and lead to apoptosis at end of S phase. Since recent literature data for dactinomycin pharmacokinetics proved to be rather scarce, a more simplistic approach has been adopted in this case as a first approximation. A cell kill fraction equal to 0.2 has been adopted as a starting point based on the fact that actinomycin- D is considered a less potent cytotoxic drug compared to vincristine, as indicated by lower AUC and higher IC50 values for various tumour and normal cells [17], [18]. Imperfect drug penetration into the tumor is assumed to have been taken into account when considering this cell kill fraction value

5) Vincristine and Actinomycin-D combined treatment.

According to the SIOP 2001/GPOH clinical trial protocol, vincristine i.v. bolus injection is directly followed by an i.v. bolus injection of actinomycin-D, with no delay in-between. Therefore, as a first approximation an additive drug effect of vincristine and actinomycin-D has been assumed. This is considered an optimal starting point for simulating the effect of practically concurrently administered drugs (when this is the case). The corresponding cell kill fractions computed according to the pharmacodynamics of each drug are added in order to acquire the total cell kill fraction (cell kill fraction = 1-cell survival fraction) [19]. The individual patient's serum immune response molecular data correlating specific tumor antigens with tumor histology (blastemal, epithelial, stromal cell fractions), which in turn considerably affects chemotherapy responsiveness, have been planned to be used in order to perturb the population based mean cell survival fractions.

C. Mesh Updating

In order to effectively simulate tumor expansion or shrinkage a provisionally acceptable upper limit (NBC$_{upper}$) and a provisionally acceptable lower limit (NBC$_{lower}$) of the number of cells contained within each GC are defined in equation (2) where fr(NBC) represents a fraction of NBC.

$$NBC_{upper} = NBC + fr(NBC)$$
$$NBC_{lower} = NBC - fr(NBC) \quad (2)$$

At each mesh scan, if the number of tumor cells contained within a given GC becomes less than NBC$_{lower}$ a procedure that attempts to "unload" the remaining cells in the neighbouring GCs that contain less than NBC cells takes place aiming at emptying the current GC. A 26 GC neighbourhood of each geometrical cell is considered. The

removed cells are preferentially placed into the neighboring GCs having the maximum available free space. If two or more of the neighboring GCs possess the same amount of free space a random number generator is used for the selection. If the given GC becomes empty it is "removed" from the tumor. An appropriate shift of a chain of GCs intended to fill in the "vacuum" leads to a differential tumor shrinkage. This can happen e.g. after a number of cells have been killed by the action of a chemotherapeutic agent.

On the other hand if the number of cells residing within a given GC exceeds NBC_{upper} a similar procedure attempting to unload the excess cells in the surrounding GCs takes place. If the unloading procedure fails to reduce the number of cells to less than NBC_{upper} then a new GC "emerges". Its position relative to the "mother" GC is determined using a random number generator. An appropriate shifting of a chain of adjacent GCs leads to a differential expansion of the tumor. The "newborn" GC contains the excess cells which are distributed in the various phase classes according to the distribution over the various phase classes in the "mother" GC.

As noted above an appropriate shifting of the contents of a chain of adjacent GCs takes place when a new GC is created or an empty GC is "removed" from the mesh. Shifting takes place along lines of random direction. This algorithm is based on the generation of random points on the surface of a hypothetical sphere centered at the GC under consideration. The shifting of the GCs takes place along the line connecting the GC under consideration and the selected random point. The discrete approximation of the line connecting the two points is computed by truncation to the nearest integer. In addition the following special morphological rule is applied. In the case of tumor shrinkage the outermost (non-empty) GC is detected along each one of among a number of lines of random directions of shrinkage. Its "6-Neighbour" GCs belonging to the Tumor (NGCT) are counted. The direction corresponding to the minimum NGCT is selected as the shifting direction. A similar, though inverse, morphologico-mechanical rule can be applied in the case of tumor expansion. These morphological rules lead to tumor shrinkage or expansion essentially conformal to the initial shape of the tumor provided that the mechanical properties of the surrounding normal tissues are assumed uniform. Conformal shrinkage due to treatment is usually the case in clinical practice. The need for the formulation of such morphological rules for tumor shrinkage and expansion has arisen from the inspection of the macroscopic results of the simulation algorithms. A completely random selection of one out of a number of shifting directions may result in a premature extensive fragmentation of the tumor region in the case of chemotherapy. This is usually incompatible with clinical experience. It should also be noted that the value of fr(NBC) influences the uniformity of the mesh in terms of cell density with a direct impact on the geometrical and volumetric aspects of the simulation. In the current version of the models fr(NBC) = NBC/10. In any case it should be noted that the underlying biology of the tumor cells is not heavily affected by the choice of fr(NBC).

III. THE NOMOGRAM OF CELL CATEGORY TRANSITION PROBABILITIES AND CELL CATEGORY RELATIVE POPULATIONS IN A FREELY GROWING TUMOR

The initialization of the tumor cell category populations plays an important role in its time evolution and the reliability of the simulation. The initial cell category relative populations or population percentages must be carefully chosen in order to obtain a tumor that develops smoothly and monotonically with time without exhibiting any peculiar behavior especially shortly after the beginning of the simulation. The effect of a wrong initialization of cell category relative populations for given cell category transition rates (or probabilities) is clarified in Fig. 3 and Fig. 4. The two sets of curves correspond to two simulations performed with the same cell category transition rates and cell cycle duration but with different initial cell category relative populations (fractions of stem, limp, diff, dead and total cells).
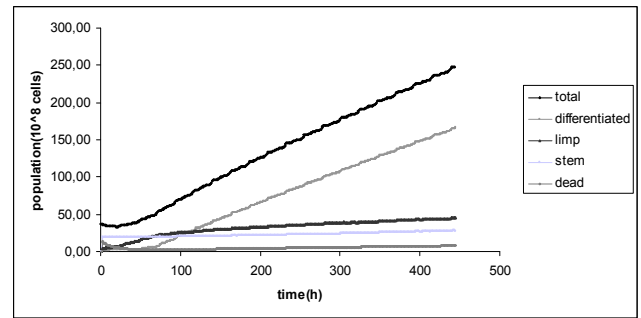

Fig. 3: Simulation predictions of free tumor growth with inappropriately chosen initial fractions of the various cell category populations (relative populations) for given transition probabilities and cell cycle duration.

However, it has been observed that even when the initial relative populations have been inappropriately chosen a more normal behavior is reached after sufficient time has elapsed. The rationale behind this is that the cell category transition probabilities determine the cell category relative populations of the tumor. In order to achieve a biologically acceptable initialization, construction of the initial tumor is achieved through initializing only one geometrical cell with a small number of stem cells. Then the simulation execution is progressing until a population of 10^6 cells within the geometrical cell is attained.
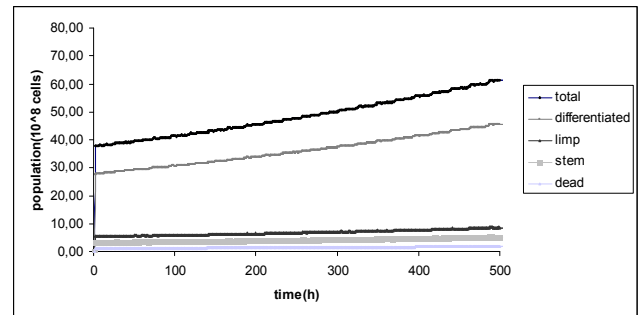

Fig. 4: Simulation results of free growth with appropriately chosen initial relative populations in relation to given transition probabilities and cell cycle duration

The cell category relative populations are then obtained and used as the basis for the initialization of each geometrical cell of the tumor. If the chosen parameters' values are not able to produce a macroscopic tumor i.e. the number of 10^6 biological cells per GC cannot be reached after a prolonged simulation period (e.g. $5*10^5$ simulated hours) the simulation exits execution. The number of stem cells to be used for the initialization of the cell category populations of the geometrical cell is chosen in such a way that a practical equilibrium of the cell category relative populations is reached before the GC is filled with 10^6 biological cells.

A number of simulation executions have been performed with different initial hypothetical populations of *stem*, *limp*, *diff* and *dead* cells in order to obtain the relative populations of the *stem*, *limp, diff* and *dead* cells after achievement of equilibrium (Table II). The latter are used for the initialization of the real tumor simulation e.g. after the treatment baseline. It is noted that in real tumors all cell category populations extant at a given (initial) time point except for the stem/clonogenic cells die and subsequently disappear. The latter are the only ones capable of regenerating the tumor on a large time scale. This is clearly demonstrated by Table II. Fig.5 shows the relative population of stem cells at equilibrium as a function of the number of stem cells used to calculate the cell category relative populations through simulation. The relative population of stem cells is expressed as a fraction of the total tumor cells. At least for the model parameter value subspace considered in this paper 1000 initial hypothetical stem cells seems to be a good choice since it ensures both achievement of equilibrium of the cell category relative populations before a total cell population of 10^6 is reached and a reasonable execution time. It is pointed out that cell category transition rates are considered approximately constant for the relatively small time interval considered by a typical simulation. Obviously cell category transition rates are expected to change dramatically with time on a much larger time scale (e.g. from the appearance of the first tumor cell till the formation of a clinically detectable tumor).

Table III presents various cell category relative (fractional) populations in near equilibrium for several values of the percentage of cells that will enter G0 following mitosis (sleep_percentage) and the percentage of stem cells that will divide symmetrically (sym_percentage). Use of fractions instead of percentages can also be made. In that case the parameters Sym_fraction and Sleep_fraction are to be used (Table IV). The parameter values shown in Table I have been used. All other cell category relative populations have been set to zero. The code was executed until the total cell population reached 10^6 cells. Each cell of limited mitotic potential (limp or progenitor cell) is assumed to undergo three mitoses before it becomes terminally differentiated.

IV. THE NEPHROBLASTOMA PARADIGM

A summary of the model parameters and their values considered are provided in Table I. Some of the parameter values such as the cell cycle duration have been based on pertinent literature whereas others have been based on both qualitative data and logic. Extensive use of pseudonymized actual SIOP 2001 / GPOH clinical trial data is expected to considerably refine the parameter value assignment. In order to simulate a realistic treatment scenario chemotherapy is assumed to start 4 days after the pretreatment imaging data are collected. Simulation continues up to 3 days after the last chemotherapy administration (Fig. 2). This also represents a real SIOP 2001 / GPOH case.

V. RESULTS

Fig. 6, Fig.7 and Fig.8 present typical tumor volume and cell population curves as functions of time for a triaxial ellipsoidal tumor with axes 10 mm, 20 cm and 30 cm. The chemotherapeutic scheme defined in Fig. 2 has been considered. A simulation execution of this treatment course takes about 3 min on a standard laptop. However there is a tremendous increase in the computational power needed with increasing spatial discrimination. During the first 4 days free growth is simulated. A monotonic increase of all cell category populations is clear during this interval. In Fig. 7 repopulation of certain cell categories can be easily observed.

TABLE I
PARAMETER VALUES USED FOR THE PRODUCTION OF THE NOMOGRAM THAT MATCHES CELL CATEGORY TRANSITION RATES AND CELL CATEGORY RELATIVE POPULATIONS FOR FREE TUMOR GROWTH

Parameter Name	Value	Definition
NBC	10^6	Number of cells contained within a geometrical cell of the mesh
T_c	23.0	Cell cycle duration (h)
max_g0_time	96	Maximum G0 phase duration before a stem or limp cell enters necrosis or re-enters cell cycle (h)
necrosis_time	20	Time before necrosis products are eliminated (h)
apoptosis_time	6	Time before apoptosis products are eliminated (h)
apoptosis_rate	0.001	Fraction of any non differentiated cell subpopulation that undergoes spontaneous apoptosis per hour (h^{-1})
diff_apoptosis_rate	0.005	Fraction of any differentiated cell subpopulation that undergoes spontaneous apoptosis per hour (h^{-1})
diff_necrosis_rate	0.001	Fraction of any differentiated cell subpopulation that eneter necrosis per hour (h^{-1})
g0_to_g1_rate	0.01	Fraction of any dormant stem or limp cell subpopulation that re-enters cell cycle per hour (h^{-1})
no_limp_classes	3	Number of mitoses that a limp (progenitor) cell should undergo before becoming terminally differentiated
margin_percent	0.1	Acceptable over-loading or under-loading of each geometrical cell of the discretizing mesh (in fraction of 1)

VI. Discussion

An advanced multilevel simulation model of clinical tumor growth and response to chemotherapy adapted to the case of nephroblastoma has been presented. More specifically a branch of the SIOP 2001 / GPOH clinical trial has been simulated. Particular emphasis has been put on the consideration of cancer stem, progenitor, differentiated and dead cells in conjunction with various metabolic states they may be found in. The need for adaptation of the cell category relative populations to the cell category transition rates has been clarified and the concept of the corresponding nomogram has been delineated. A technique to initialize the various cell category relative populations at the beginning of the simulation has been described and its convergence has been studied. Indicative results have been presented for a pertinent subspace of the parameter values combinations. Based on Table III it appears that the stem cell percentage (stem cell relative population) depends strongly on the symmetric division probability. On the other hand the progenitor cell relative population depends strongly on both the symmetric division probability and the number of stem cells. An increasing symmetric division probability leads to an increase of the progenitor cell relative population. However after a turning point it leads to a decrease of the progenitor cell relative population. Similar remarks can be made and explained for other parameters interdependences. Furthermore, the simulation outcomes presented for free tumor growth (Fig. 4) and response to chemotherapy (Fig. 6-8) are in agreement with clinical experience at least qualitatively. Consideration of a macroscopically layered tumor [3-5] and assignement of different cell category transition rates in its dynamically changing layers is expected to improve the model's predictive potential in those cases. An extensive use of SIOP 2001 / GPOH clinical trial data is also expected to considerably refine the assignment of certain model parameter values.
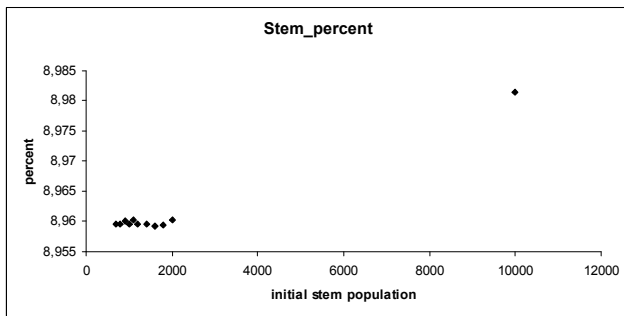

Fig. 5.: Relative population of stem cells at equilibrium as a fuction of the number of initial stem cells used to produce the relative populations of each cell category at the treatment simulation starting point. The relative population of stem cells is expressed as a percentage of the total tumor cells (abbreviated here as "percent"). It can be noticed that if less than 2000 initial stem cells are used to produce all cell category relative populations and therefore initialize the clinical tumor good stabilization of the stem cell relative population is achieved (for the subspace of parameter values combinations addressed here).

TABLE II
POPULATIONS OF STEM, LIMP (PROGENITOR), DIFFERENTIATED AND DEAD CELLS USED TO INITIALIZE THE PROCEDURE FOR THE CALCULATION OF THE RELATIVE POPULATIONS (PERCENTAGES OF TOTAL CELLS) OF SEVERAL TUMOR CELL CATEGORIES

Stem_population	Limp_population	Diff_population	Dead_population	Stem_percentage	Limp_percentage	Diff_percentage	Dead_percentage
700	0	0	0	8.959	14.551	73.634	2.854
800	0	0	0	8.959	14.551	73.634	2.854
900	0	0	0	8.960	14.552	73.630	2.854
1000	0	0	0	8.959	14.551	73.634	2.854
1100	0	0	0	8.960	14.552	73.632	2.854
1200	0	0	0	8.959	14.551	73.634	2.854
1400	0	0	0	8.959	14.551	73.634	2.854
1600	0	0	0	8.959	14.550	73.635	2.854
1800	0	0	0	8.959	14.551	73.634	2.854
2000	0	0	0	8.960	14.552	73.633	2.854
10000	0	0	0	8.981	14.587	73.583	2.840
1000	1000	0	0	8.9595	14.551	73.634	2.854
1000	1000	1000	1000	8.9595	14.551	73.634	2.854
1000	3000	5000	10000	8.9595	14.551	73.634	2.854

TABLE III
PART OF THE NEPHROBLASTOMA NOMOGRAM

Sleep_percentage	Sym_percentage	Stem_fraction	Limp_fraction	Diff_fraction	Dead_fraction
0	10	0.019	0.098	0.862	0.020
	20	0.046	0.168	0.768	0.018
	30	0.085	0.224	0.675	0.016
	40	0.14	0.268	0.578	0.014
	50	0.213	0.292	0.483	0.013
	60	0.308	0.294	0.387	0.011
	70	0.43	0.27	0.29	0.01
	80	0.581	0.215	0.194	0.01
	90	0.767	0.128	0.097	0.008
	100	0.992	0	0	0.008
10	20	0.032	0.118	0.827	0.023
	30	0.072	0.191	0.715	0.022
	40	0.127	0.244	0.609	0.02
	50	0.202	0.275	0.505	0.018
	60	0.297	0.283	0.403	0.017
	70	0.419	0.263	0.302	0.016
	80	0.571	0.212	0.201	0.016
	90	0.759	0.126	0.1	0.015
	100	0.986	0	0	0.014
20	30	0.042	0.11	0.823	0.026
	40	0.103	0.195	0.677	0.025
	50	0.179	0.245	0.551	0.025
	60	0.278	0.264	0.434	0.024
	70	0.403	0.252	0.322	0.023
	80	0.557	0.207	0.213	0.023
	90	0.747	0.124	0.106	0.023
	100	0.978	0	0	0.022
30	50	0.117	0.16	0.693	0.03
	60	0.232	0.221	0.517	0.03
	70	0.367	0.23	0.372	0.031
	80	0.531	0.197	0.241	0.031
	90	0.73	0.121	0.118	0.031
	100	0.969	0	0	0.031
40	80	0.45	0.167	0.343	0.05
	90	0.688	0.114	0.156	0.042
	100	0.957	0	0	0.043

Parameter name	Value	Definition
Sym_fraction	0.45	Fraction of stem cells that divide symmetrically.
Sleep_fraction	0.28	Fraction of cells that will enter G0 following mitosis
Stem_fraction	0.09	Fraction of total cells that are stem cells
Limp_fraction	0.15	Fraction of the total cells that are limp cells
Diff_fraction	0.73	Fraction of total cells that are differentiated cells
Dead_fraction	0.03	Fraction of total cells that are dead
a_fraction	0.61	Fraction of dead cells that are apoptotic
n_fraction	0.39	Fraction of dead cells that are necrotic
Limp1_fraction	0.23	Fraction of limp cells that have not undergone any mitoses
Limp2_faction	0.32	Fraction of limp cells that have undergone 1 mitosis
Limp3_fraction	0.45	Fraction of limp cells that have undergone 2 mitoses
G0_fraction	0.1	Fraction of the sum of proliferating and dormant cells that are dormant
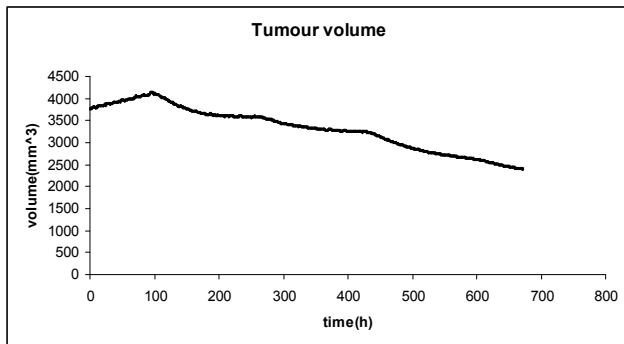
Fig. 6: Nephroblastoma tumor volume as a function of time for the chemotherapeutic treatment of Fig.1. The parameter values included in Table I have been used. At time t=0 the three axes of the ellipsoidal tumor are 10 mm, 20 mm and 30 mm.
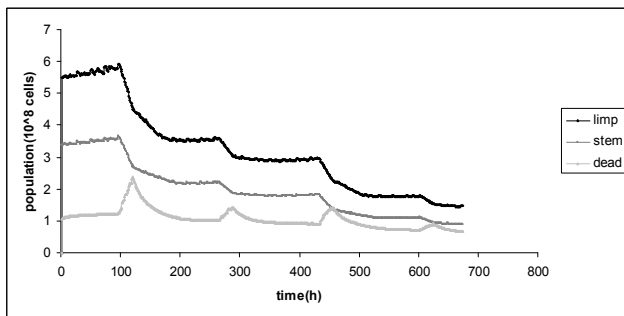

Fig. 7. Time course of the proliferating (stem and progenitor) and dead cells for the tumor considered in Fig. 6
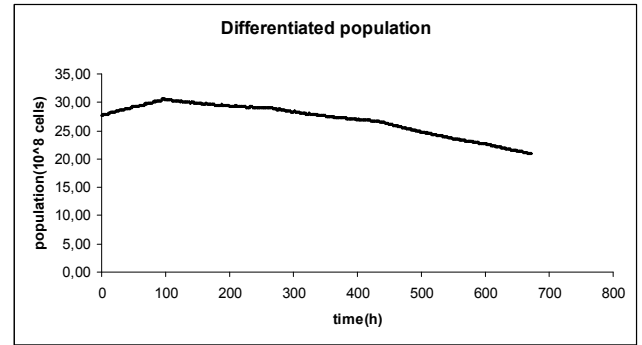

Fig. 8: The time course of the differentiated cell population of the tumor considered in Fig. 6

It should be stressed that although the number of independent model parameters is considerable, the requirements concerning satisfaction of the biological boundary conditions, limit the number of biologically acceptable solutions. In any case developing a multi-scale tumor dynamics model dictates the incorporation of a substantial number of parameters so that an extensive exploitation of experimental and clinical information can be achieved.

VII. CONCLUSION

A clinically oriented multiscale discrete state spatiotemporal model of the response of solid tumors such as nephroblastoma to chemotherapeutic treatment has been delineated. Special emphasis has been put on the consideration of the stem, progenitor, differentiated and dead cancer cells. The need for matching of the cell category transition rates with the cell category relative populations at the start of simulation of free growth for an already large solid tumor has been clarified. A technique to ensure satisfaction of this condition has been suggested and succesfully applied. A preliminary analysis of the model's behavior for a pertinent subspace of the parameter values combinations has been carried out. A thorough sensitivity and parameter interdependence analysis of the model in order to determine its behavior in the extremes of its parameter value space is in progress. However for the typical parameter values considered the model behaves at least in qualitative agreement with clinical reality. Quantitative clinical adaptation in conjunction with the exploitation of serum molecular data (the "antigen scenario") reflecting the tumor's histology as well as extensive validation of the model within the framework of the ACGT propject are in progress. A patient individualized decision support system which would lead to treatment optimization through performing experiments *in silico* (on the computer) is expected to be one of the end products of the project. Such a system might also serve as both a basic research tool and an educational platform.

REFERENCES

[1] ACGT: Advancing Clinicogenomic Trials on Cancer (FP6-2005-IST-026996), http://www.eu-acgt.org/

[2] N. Graf and A. Hoppe, "What are the expectations of a Clinician from *In Silico* Oncology ?," *Proc. 2nd International Advanced Research Workshop on In Silico Oncology*, Kolympari, Chania, Greece, 25-26 Sept. 2008, Ed. K. Marias and G. Stamatakos, pp. 36-38 (http://www.ics.forth.gr/bmi/2nd-iarwiso/)

[3] G.S. Stamatakos, D.D. Dionysiou, E.I. Zacharaki, N.A. Mouravliansky, K.S.Nikita, N.K. & Uzunoglu , In silico radiation oncology: combining novel simulation algorithms with current visualization techniques , *Proceedings of IEEE:* Special Issue on Bioinformatics: Advances and Chalenges , 90(11) , 1764-1777 , 2002.

[4] D. D. Dionysiou, G. S. Stamatakos, N.K. Uzunoglu, K. S. Nikita, A. Marioli, "A four-dimensional simulation model of tumour response to radiotherapy in vivo: parametric validation considering radiosensitivity, genetic profile and fractionation," *Journal of Theoretical Biology* vol. 230, pp. 1–20, 2004

[5] G. S. Stamatakos, V. P. Antipas and N. K. Uzunoglu, "A spatiotemporal, patient individualized simulation model of solid tumor response to chemotherapy in vivo: the paradigm of glioblastoma multiforme treated by temozolomide," *IEEE Transactions on Biomedical Engineering*, vol. 53, pp. 1467- 1477, 2006

[6] G.S.Stamatakos, D.D.Dionysiou, N.M.Graf, N.A.Sofra, C.Desmedt, A.Hoppe, N.Uzunoglu, M.Tsiknakis , "The Oncosimulator: a multilevel, clinically oriented simulation system of tumor growth and organism response to therapeutic schemes. Towards the clinical evaluation of *in silico* oncology," *Proceedings of the 29th Annual International Conference of the IEEE EMBS*, August 23-26, SuB07.1: 6628-6631 , Lyon, France , 2007

[7] Lodish D. Baltimore, A. Berk, S. Zipursky, P. Matsudaira, and J. Darnell*, Molecular Cell Biology*. New York: Scientific American Books, 1995, pp. 1247–1294.

[8] Perez and L. Brady, Eds.*, Principles and Practice of Radiation Oncology*.

[9] G. Steel, Ed.*, Basic Clinical Radiobiology*, 3rd ed. London, U.K.: Arnold, 2002, pp. 165–168, pp. 13, 52–63.

[10] S.E.Salmon and A.C.Sartorelli "Cancer Chemotherapy", in *Basic & Clinical Pharmacology*, B.G.Katzung, ed. Lange Medical Books/McGraw-Hill, International Edition, 2001, pp.923-1044.

[11] E. Groninger, T. Meeuwsen-de Boer, P. Koopmans, D. Uges, W. Sluiter, A. Veerman, W. Kamps, S. de Graaf. Pharmacokinetics of Vincristine Monotherapy in Childhood Acute Lymphoblastic Leukemia. *Pediatric Research* vol. 52: pp. 113-118, 2002.

[12] W.N. Dahl, R. Oftebro, E.O.Pettersen, T. Brustad, "Inhibitory and cytotoxic effects of Oncovin (Vincristine Sulfate) on cells of human line NHIK 3025," *Cancer Res*. vol. 36, pp. 3101-3105, 1976.

[13] W.T.Beck, C.E.Cass, P.J.Houghton. "Microtubule-targeting anticancer drugs derived from plants and microbes: Vinca alkaloids, taxanes and epothilones," In: Holland JF, Frei E III, Bast RC Jr, Kufe DW, Morton DL, Weichselbaum RR, eds. Cancer Medicine, 5th Edition. Atlanta: American Cancer Society; 2000 pp. 680-698.

[14] K.W.Wood, W.D.Cornwell, J.R.Jackson, " Past and future of the mitotic spindle as an oncology target," *Current Opinion in Pharmacology* vol. 1(4), pp. 370-377, 2001.

[15] C. R. Pinkerton, B. McDermott, T. Philip, P. Biron, C. Ardiet, H. Vandenberg, and M. Brunat- Mentigny, "Continuous vincristine infusion as part of a high dose chemoradiotherapy regimen: drug kinetics and toxicity," *Cancer Chemother Pharmacol* 22: 271-274, 1988.

[16] H. Kobayashi, Y.Takemura, JF. Holland, T.Ohnuma, "Vincristine saturation of cellular binding sites and its cytotoxic activity in human lymphoblastic leukaemia cells, " *Biochem. Pharmacol.* vol. 55, pp. 1229-1234, 1998.

[17] K.Sawada, K.Noda, H. Nakajima, N. Shimbara, Y.Furuichi, M. Sugimoto, "Differential cytotoxicity of anticancer agents in pre- and post-immortal lymphoblastoid cell lines," *Biol Pharm Bull* vol. 28, pp. 1202-1207, 2005.

[18] G.J.Veal, M. Cole, J.Errington, A.Parry, J.Hale, A.D.J.Pearson, K.Howe, J.C.Chiholm, C.Beane, B.Brennan, F.Waters, A.Glaser, S.Hemsworth, H. McDowell, Y.Wright, K.ritchard- Jones, R.Pinkerton, G.Jenner, J.Nikolson, A.M.Elsworth, A.V.Boddy, and UKCCSG Pharmacology Working Groups, "Pharmacokinetics of Dactinomycin in a pediatric patient population: a United Kingdom Children's Cancer Study group study," *Clin Cancer Res* vol. 11(16), pp. 5893-5899, 2005.

[19] C.D.Scripture and W.D.Figg, "Drug interactions in cancer therapy," Nat Rev Cancer 6, pp. 546-558, 2006.